Diamond & Related Materials 77 (2017) 84–91

Contents lists available at ScienceDirect

Diamond & Related Materials

journal homepage: www.elsevier.com/locate/diamond

Tribological properties of hydrogenated amorphous carbon films in different atmospheres

Jing Shi[a,b], Zhenbin Gong[a,b], Chengbing Wang[c], Bin Zhang[a,d,*], Junyan Zhang[a,**]

[a] State Key Laboratory of Solid Lubrication, Lanzhou Institute of Chemical Physics, Chinese Academy of Sciences, Lanzhou 730000, China
[b] University of Chinese Academy of Sciences, Beijing 100049, China
[c] School of Materials Science & Engineering, Shaanxi University of Science and Technology, Xi'an, Shaanxi 710021, China
[d] Lawrence Berkeley National Laboratory, Berkeley, CA 94720, USA

ARTICLE INFO

Keywords:
Diamond like carbon film
Atmosphere
Adsorption
Superlubricity

ABSTRACT

In this study, hydrogenated amorphous carbon (a-C:H) films prepared by plasma enhanced chemical vapor deposition had distinguishing tribology behaviors in dry nitrogen, oxygen, argon, humid air and vacuum. Both the friction and wear rates of a-C:H films sliding against Al_2O_3 in nitrogen and argon were lower than that in oxygen and humid air atmospheres. And superlubricity (0.009) was achieved in dry nitrogen atmosphere for self-mated a-C:H counterpart. From the viewpoint of various gas molecules' adsorption, the a-C:H films' friction behavior was investigated. Micro-Raman and scanning electron microscope (SEM) were employed to study the interfacial structural evolution and tribofilm distribution in different atmospheres. X-ray photoelectron spectroscopy (XPS) was used to reveal the relation between wear rate and tribo-oxidation reaction in various atmospheres. We confirmed that nitrogen molecule provided repulsion force at sliding interface and reduced friction of a-C:H film. Meantime, graphitic tribofilm also played a significant role. It was stated that electronic repulsion force aroused by adsorption was enough for ultra-low friction, while the presence of graphitic tribofilm had synergetic effect with it in achieving superlubricity. This study provided considerations and discussions about interfacial electronic character's effect on friction behaviors of carbon based film.

1. Introduction

Friction and wear are the majority of energy consumption on moving mechanicals in industry [1–3]. This triggers tribologists to find ways, like designing new lubricating oils, nano-lubricant-additives and solid coatings, to save energy via reducing friction and wear. Interestingly, diamond-like carbon (DLC) films are employed as excellent solid lubricants in various environments to achieve superlubricity over the past few decades [4–9]. However, friction of DLC film is sensitive to its working environments, such as atmospheres, relative humidity etc. [5,10,11]. Usually, hydrogen free amorphous carbon (a-C and ta-C) film's friction coefficient (Cof.) is mainly controlled by the surface unterminated dangling bonds, and its corresponding friction mechanism is of less controversy [12,13]. In inert gas and vacuum environments, large amount of dangling σ bonds in a-C/ta-C films can cause severe adhesion at frictional interface. Under these conditions, the friction coefficient could be the same as diamond's (~0.3) [14]. With the increase of relative humidity, water molecules can terminate the dangling bonds which in turn lower the friction immensely [15–17]. However, hydrogenated amorphous carbon (a-C:H) films have more complex tribological properties due to its structural diversity and environmental sensitivity. For instance, in vacuum condition, hydrogen saturation dangling bonds is beneficial to the (super-) low friction of a-C:H [4,5,18,19], though the friction coefficient can vary within one order of magnitude as the vacuum pressure increased in a specific range [20]. But the presence of water molecules can destroy super-low friction of a-C:H films [21,22].

Although the vacuum and pure inert atmospheres are similar in the amount of active species, a-C:H film's friction behaviors are different in these two conditions. Studies showed that a-C:H film had exceptional tribological property in inert atmosphere [23], but its wear life was strongly restricted in vacuum [20,24]. Accordingly, referred to the friction and wear properties, role of gas molecules on sliding interfacial of a-C:H films should be taken into full consideration. Besides, gas molecules that follows Elovich equation could have interaction with a-C:H film' surface to form gas layers, which suggested that the electronic character of frictional interface should not be overlooked as well [25,26]. In this study, the tribological properties of a-C:H films were

* Correspondence to: B. Zhang, State Key Laboratory of Solid Lubrication, Lanzhou Institute of Chemical Physics, Chinese Academy of Sciences, Lanzhou 730000, China.
** Corresponding author.
E-mail addresses: bzhang@licp.cas.cn (B. Zhang), zhangjunyan@licp.cas.cn (J. Zhang).

http://dx.doi.org/10.1016/j.diamond.2017.06.005
Received 18 January 2017; Received in revised form 12 June 2017; Accepted 12 June 2017
Available online 15 June 2017

investigated in dry nitrogen, argon, oxygen, humid air and high vacuum atmospheres. Self-mated a-C:H films achieved superlubricity in dry nitrogen atmosphere, which is different from that in high vacuum and humid air (relative humidity ~37%). Synergistic effect of intrinsic H, graphitic tribofilm and repulsion force was fully discussed.

2. Experimental details

2.1. Preparation of a-C:H films

The as-deposited a-C:H films were prepared by plasma enhanced chemical vapor deposition system using CH_4 and Ar as precursors. Details about this system were described elsewhere [27]. A-C:H films were deposited on monocrystalline silicon wafers and α-Al_2O_3 balls (diameter of 5 mm). The silicon wafers were directly put on the cathodic sample table and the Al_2O_3 balls were fixed onto stainless steel holder using conducting resin and then put on the sample table. All the substrate materials were carefully cleaned before they were moved into the depositing chamber. During the depositing, direct current negative bias of −1000 V was applied and 30 sccm CH_4 and 200 sccm Ar were fed as process gases (working pressure was kept constant at 18 Pa). Power frequency and duty cycle were 60 KHz and 60%, respectively.

2.2. Friction tests and structural analysis

Friction tests were performed on a ball-on-disk tribo-meter, which was entirely installed in a chamber connected with pump system and additional gas controlling part. Bare Al_2O_3 balls and a-C:H coated Al_2O_3 balls were both employed to slide against a-C:H films (deposited on silicon wafers). Applied normal load was 20 N. Commercial high-purity dry nitrogen, oxygen and argon gases were employed to drive gaseous atmospheres. And the vacuum friction tests were performed under vacuum pressure of 2×10^{-4} Pa. The revolution diameter was 3 mm and the linear speed was 31 mm/s. Each of the friction tests was repeated at least three times to ensure veracity. The friction coefficients in Fig. 3 were the calculated average values.

Frictional interface morphology was observed by optical microscope (Olympus, DP73) and scanning electron microscope (SEM, JSM-5601LV). The a-C:H film's cross sectional image was also measured by SEM method, and the film thickness was calculated by the average values at five different places. Micro-Raman (LabRam HR800, laser wavelength of 532 nm) and X-ray photoelectron spectroscopy (XPS, Thermo Fisher Scientific, ESCALAB 250Xi) were employed to investigate the wear tracks and wear scars structure and chemical composition before and after the friction tests. Cross section profiles of wear tracks were measured by two-mode three-dimensional surface contour graph (AEP). Surface roughness root mean square of as-deposited a-C:H film was observed by atomic force microscope (AFM, SPM-9500). The film hardness and elasticity were tested on Ti-950 nano-indentation. The a-C:H films with thickness less than 30 nm, deposited on NaCl and then dispersed in distilled water to transfer onto Cu grids, was used for high resolution transmission electron microscopy (TEM, JEOL 2010) analysis.

3. Results and discussions

The as-deposited a-C:H film on silicon substrate was ~634 nm in thickness with hardness of 14.6 GPa and elasticity of 78% (Fig. 1a and b). The film showed amorphous character according to its high resolution TEM image and selected area electron diffraction pattern (Fig. 1c). Micro-Raman spectrum was employed for a further structural confirmation due to its effectiveness in distinguishing carbon bonding types. Usually, amorphous carbon structure has micro-Raman spectra that involves a G peak centered at around 1560 cm^{-1} wavenumber and a D peak at around 1350 cm^{-1} [28]. In this study, the as-deposited a-C:H film showed typical amorphous characteristic according to its Raman spectrum and Gaussian fitting results: a G peak centered at 1540 cm^{-1} and a shoulder D peak at 1365 cm^{-1} (Fig. 1d).

3.1. Friction and wear behaviors of a-C:H films

It is of less controversy that friction behaviors of diamond like carbon films are simultaneously affected by intrinsic features and environmental factors [29]. The a-C:H films' friction tests were performed in inert atmospheres (nitrogen and argon), active atmosphere (oxygen) and humid air (relative humidity ~37%). It can be observed from Fig. 2 that the friction of the a-C:H is closely related to environmental gas species. Friction coefficient of a-C:H in inert species (N_2 and Ar) is lower than that in active atmospheres (O_2 and humid air). Also, in Fig. 2, each of the friction curves has incipient high friction in run-in period and then transits into a steady state [30]. Usually, film roughness and surface oxides were dominant for the run-in period [31,32]. The a-C:H film's surface roughness RMS is 3.3 nm only (see Fig. S1), so the steady state friction under four atmospheres was achieved within 600 sliding cycles (Fig. 2).

The a-C:H film exhibited stable and low friction in dry nitrogen and dry argon environments after a run-in time. However, the friction curves fluctuate in oxygen and humid air and the friction coefficient was higher than that in nitrogen and argon. Intrinsically, carbon film with higher H content usually behaves lower friction in vacuum according to previous study [33]. However, friction results here indicate that apart from the intrinsic hydrogen content, gas atmospheres also have pronounced effect on friction of a-C:H film. Besides, wear track in nitrogen was more inconspicuous than that in oxygen and argon, and the width was 154 μm, 156 μm, 123 μm and 167 μm in nitrogen, argon, oxygen and humid air, respectively (Fig. 2 insets). The average values of friction coefficient at steady state and wear rates calculated from the wear tracks are shown in Fig. 3. It can be seen that coefficient in nitrogen (0.017) is lower than that in argon (0.023) and in oxygen (0.069). Similar variation can be found in their corresponding wear rates. The wear track in nitrogen is faint and corresponds to the lowest wear rate ($1.2 \times 10^{-8} mm^3N^{-1}m^{-1}$). In argon and oxygen, the wear rates are $2.1 \times 10^{-8} mm^3N^{-1}m^{-1}$ and $6.0 \times 10^{-8} mm^3N^{-1}m^{-1}$, respectively. However, in humid air, the a-C:H film friction (0.12) and wear rate ($6.2 \times 10^{-8} mm^3N^{-1}m^{-1}$) are the highest. The wear tracks' sectional profiles were shown in Fig. S2. One possible reason for this is the inert gas molecules can eliminate the shear force produced σ bonds through physical adsorption [34]. And in humid air, water molecules have negative effect on friction coefficient, because the adsorption of water usually form the COO– followed by C—O bonds. And this accelerates the break of bulk carbon networks in a-C:H films [35]. Moreover, interfacial nano-scale adhesion aroused by capillary force is also important because the a-C:H film is relative hydrophilic [36,37]. But water molecules are isolated in high-purity dry nitrogen, oxygen and argon atmospheres. Therefore, friction in humid air (Cof. = 0.12) was higher than that in these three atmospheres.

Gas molecules' adsorption modes on a-C:H film have a close relation with its friction behaviors [26]. Different gas molecules have distinct effects on carbon film surface, which can explain the friction differences in nitrogen and argon atmospheres. Another proof that the gas atmosphere and bulk H have synergistic effect on the a-C:H film friction was shown in Fig. 4. Assuming that gas molecules were incapable of adsorbing on a-C:H surface physically or chemically, then it can be deduced that the friction in vacuum and inert atmospheres would be only terminated by bulk hydrogen as an internal factor. As a result, their friction coefficient should be almost the same. In fact, the friction coefficient and wear rate of a-C:H film sliding against bare Al_2O_3 in high vacuum was 0.1 and $5.6 \times 10^{-8} mm^3N^{-1}{\cdot}m^{-1}$, respectively (Fig. 4 and Fig. S2e). In vacuum, the friction freed dangling bonds were directly brought into contact and aroused strong interfacial adhesion [34]. The bulk stock H can partly terminate the dangling bonds; therefore, coefficient and wear rate in vacuum are higher than that in

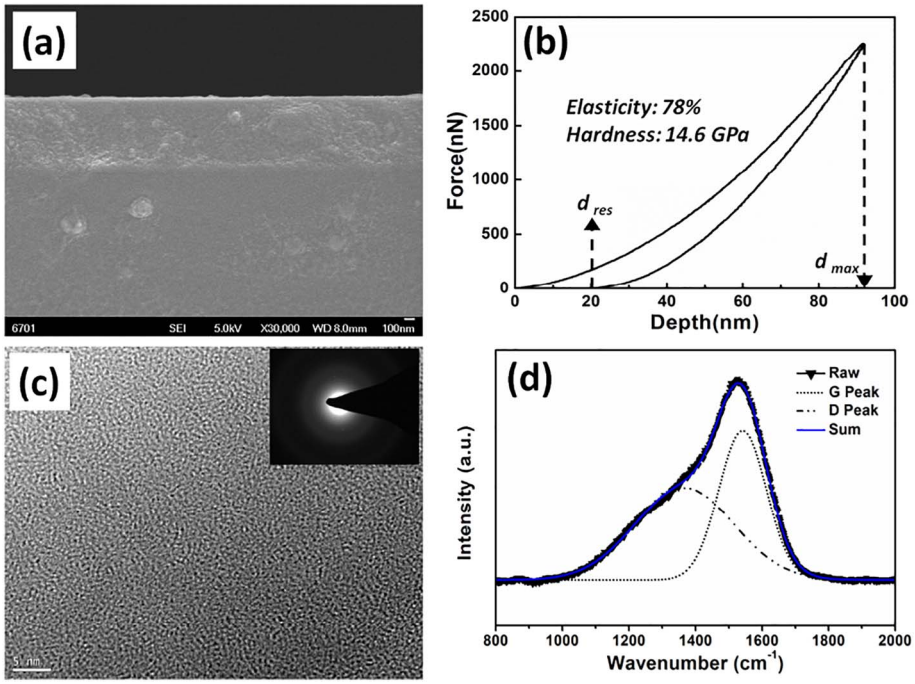

Fig. 1. (a) Sectional scanning electron microscope picture, (b) typical loading-unloading curve, (c) high resolution TEM picture and (d) selected area electron diffraction pattern of the a-C:H film.

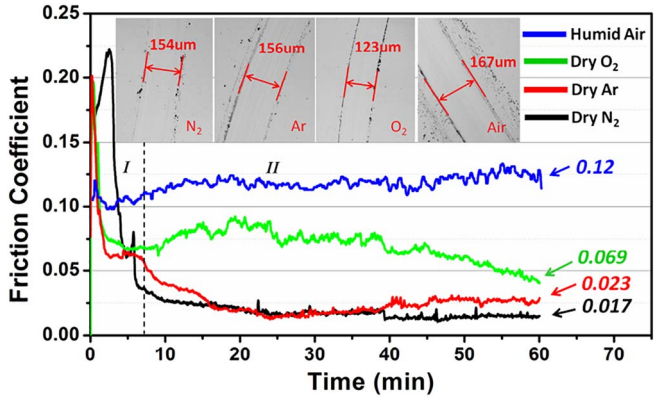

Fig. 2. a-C:H film's friction curves in N_2, O_2, Ar and humid air (relative humidity ~37%). The insets are the corresponding optical graphs of wear tracks after friction. The steady state friction coefficient is labeled at the end of each curve.

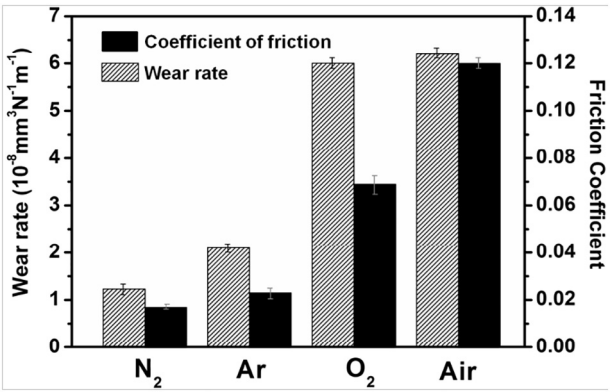

Fig. 3. Average friction coefficient and wear rates of a-C:H/Al_2O_3 counterparts in Ar, N_2, O_2 and humid air (relative humidity ~37%).

N_2 and Ar atmospheres [38]. Hence, when the a-C:H was exposed in various atmosphere (N_2, O_2 and Ar), these molecules were adsorbed to form a gas layer that follows the Elovich equation [25,26]. Even if the gas layer was destroyed by interfacial shear, adsorption process would

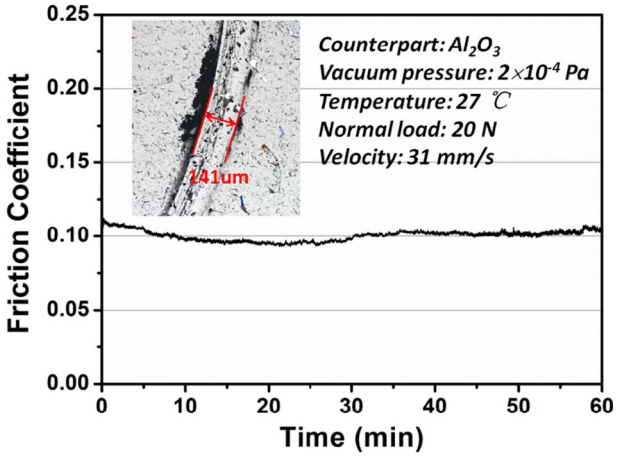

Fig. 4. Friction curve of the a-C:H/Al_2O_3 counterpart in high vacuum. The inset is the optical graph of wear track after friction.

continuously conduct to form a new layer. But what is the reason for the distinction of friction coefficient in N_2, O_2 and Ar? According to J.A. et al. [25,39], when N_2 molecules were physically adsorbed onto surface C—H bonds, one pair of free electrons in N_2 would interact with H, which enables the adsorbed N_2 molecules to stay in a relative rich-electron state and to act as electron donators. When the twofold a-C:H films were brought into contact, this rich-electron state could arouse electrostatic repulsion at frictional interface. In brief, in dry nitrogen, the low friction of a-C:H could be understood by the electrostatic repulsion mechanism. For argon atmosphere, adsorption was barely realized because Ar is monatomic molecule with stable electron structure, which would not have electron cloud interaction with C and H atoms. Therefore, the friction coefficient of a-C:H film in Ar was higher than that in dry N_2. Unlike physically adsorbed nitrogen molecules, the oxygen molecules are chemically adsorbed onto a-C:H film surface with higher binding energy [40–42]. Wang et al. proved that single O atom would react with diamond-like carbon surface to form C—O—C bonds and lead to strong adhesion at sliding interface [41], which is contrary to nitrogen molecules' role in reducing friction of the a-C:H film. Therefore, the contact interface was switched to high friction regime in

the presence of oxygen molecules. Moreover, during the run-in period in Fig. 2 (stage *I*), N_2 molecules desorption rate on a-C:H film surface might be larger than the adsorption rate [43–45]. So in this stage, the friction coefficient was high and unstable. When it comes into stable period (stage *II* in Fig. 2), the wear off of surface multi-asperity promoted the tribofilm formation and the balance between desorption and adsorption was achieved [46]. In this stage, the interfacial electron character was predominant for the friction. Therefore, in nitrogen and argon the friction was more stable and lower than that in humid air and oxygen (Fig. 2).

Although the a-C:H/Al_2O_3 counterpart has been proved to exhibit low friction in high purity nitrogen atmosphere, the adsorption capacity still differs on these two counterfaces. If the proposed adsorption mechanism works at a-C:H/Al_2O_3 interface, then one can conclude that the self-mated a-C:H/a-C:H counterparts would have ultra-low friction in nitrogen, either. Because the electrostatic repulsion at self-mated interface was stronger than that of a-C:H/Al_2O_3. As has discussed above, the weak shear force aroused by electrostatic repulsion was formed at frictional interface of Al_2O_3/a-C:H. In this case, the electrostatic repulsion was mainly between the adsorbed nitrogen molecules and Al_2O_3 surface as well as the surrounding N_2 molecules. However, for the condition of self-mated a-C:H/a-C:H counterparts, both of the two counterfaces were available for adsorption, which severely increased the interfacial repulsion force. Therefore, superlubricity could be achieved. This hypothesis was identified by friction test shown in Fig. 5. The a-C:H films were deposited on both Al_2O_3 and Si to obtain self-mated a-C:H counterfaces. After a run-in period, superlubricity (Cof. = 0.009) was reached. Moreover, the wear rate calculated from the wear track profile (Fig. S2f) was $6.2 \times 10^{-9} mm^3 N^{-1} m^{-1}$, which is even lower than that of a-C:H/Al_2O_3 counterface in nitrogen. Hitherto, systematic friction tests reveal that electrostatic repulsion force aroused by nitrogen molecules' adsorption has a significant effect on a-C:H film's superlubricity. And the severe interfacial adhesion aroused by O_2 chemical adsorption was predominant for the high friction coefficient of a-C:H film.

3.2. Micro-Raman characters of tribofilm

Carbon atoms in a-C:H film were connected by σ and π bonds, which were thermodynamically non-equilibrium according to the atomic and electronic structure model proposed by Robertson [47,48]. Graphitization [49] process under shear stress usually signifies that proportional sp^3-C phase transformed into sp^2-C phase, which was thermodynamically more stable. In previous studies [50,51], this process was proved to be associated with film bulk atoms' rearrangement and saturation of dangling bonds (freed by the shear stress) by environmental species. This tribo-induced hybridization change was even detected in

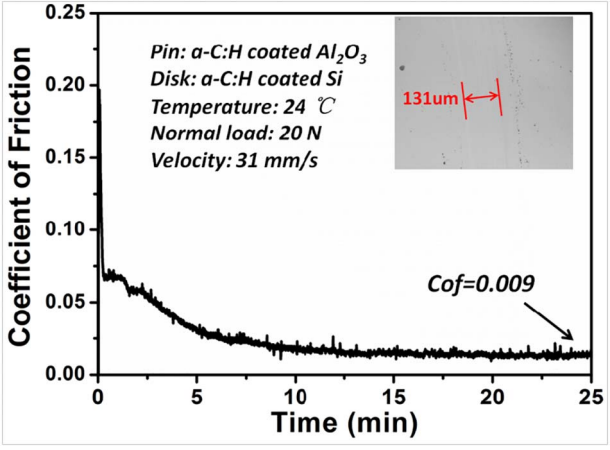

Fig. 5. Friction curve of self-mated a-C:H films in N_2 atmosphere.

mild condition for nanocrystalline diamond [52]. In brief, friction induced graphitization process could be described as follows: at first step the film bulk hydrogen atoms released and leaded to film lattice relaxation and then shear deformation promoted the formation of graphitic phase [53].

Fig. 6 shows the ensemble of Raman spectra (532 nm): as-deposited a-C:H film, friction interface including wear scars on Al_2O_3 and wear tracks on a-C:H. It was revealed that the as-deposited film had typical Raman characteristic of amorphous carbon structure: G peak centered at 1540 cm^{-1} and a broad shoulder peak at around 1365 cm^{-1} (see fitting results in Fig. 1d). While after the friction in nitrogen atmosphere, Raman spectrum of wear scar center showed obvious change (Fig. 6a): D peak intensively aroused and G peak became sharper and peak center moved to higher wavenumber. Similar Raman change was also found in a-C:H wear track center in nitrogen (Fig. 6a). These two additional sharp and narrow peaks could be assigned to D_{GR} (1330 cm^{-1}) and G_{GR} (1580 cm^{-1}) [52]. G E_{2g} symmetry breathing represented the in-plane stretching breathing mode of sp^2-C pair-atoms in aromatic and olefinic molecules more than in six-fold rings. While the symmetry breathing D band intensity arouse signifies the presence of sp^2 atoms in clusters or six-fold aromatic rings in disordered structure [52,54]. But the peak width is broader than that of perfect graphite, which reveals a long range disordered characteristic compared to perfect nano-graphite [55]. Besides, in the case of self-mated a-C:H counterparts in nitrogen (Fig. 6d), D and G peak locations of wear scar center were one-to-one corresponding to 1330 cm^{-1} and 1580 cm^{-1}. Clearly, Raman spectra variation in N_2 friction indicates that the wear scar centers (a-C:H/Al_2O_3 and twofold a-C:H) were covered with friction induced graphitic tribofilm that experienced transformation from sp^3-C phase into sp^2-C phase. Similarly, in dry oxygen friction, the Raman spectra of wear track and wear scar edge also showed D_{GR} and G_{GR} arousing (Fig. 6b). However, it was noticeable that the Raman spectra of wear scar centers (real contact area) in both oxygen and argon only showed typical peaks of Al_2O_3 (Fig. S3), which directly reveals that the tribofilm was destroyed in these two atmospheres. In other words, in oxygen and argon atmospheres, the wear scar centers were bare with no tribofilm. Overall, superlubricity was only achieved in nitrogen, but the friction coefficient in argon was 0.023. It can be concluded that the electronic repulsion force aroused by adsorption was enough for ultra-low friction, while the presence of graphitic tribofilm had synergetic effect with it in achieving superlubricity.

In dry nitrogen, wear debris from a-C:H/Al_2O_3 counterpart were discontinuously wrinkled at the wear scar center and small amount of shelled particles were distributed at wear scar edge (Fig. 7a). When the a-C:H coated Al_2O_3 balls were sliding against a-C:H films in dry nitrogen, the corresponding wear debris were rod-like (Fig. 7d). While for the condition of a-C:H/Al_2O_3 counterpart in oxygen and argon, a great deal of cotton-like particles distributed at the wear scar edges could be observed from the enlarged views (insets in Fig. 7b, c). As shown in Fig. 6, wear scars edges of bare Al_2O_3 in oxygen, argon and the a-C:H coated Al_2O_3 in nitrogen all showed graphitic characteristic, but this feature was only achieved at wear scar center areas in dry nitrogen. Another significant factor for the formation of tribofilm was the low shear force provided by adsorbed N_2 molecules on a-C:H surface as was discussed before. More specifically, self-mated a-C:H counterparts in dry nitrogen generated dipoles at interface to protect the existence of tribofilm. However, in the case of oxygen, the tribofilm was destroyed and sprayed to wear scar edge due to strong interfacial adhesion effect aroused by chemical adsorption. Similarly, the pin and disk were brought into direct contact and the formation of tribofilm at wear scar center was also prevented in argon atmosphere. Hence, these two factors could explain why superlubricity was only achieved for self-mated a-C:H counterparts in dry nitrogen (Cof. = 0.009). In conclusion, combined with the tribofilms' structure (Raman) and distribution (SEM) analysis, it is clear that the graphitic tribofilm was destroyed in the presence of oxygen and argon. The wear debris was formed by peeling

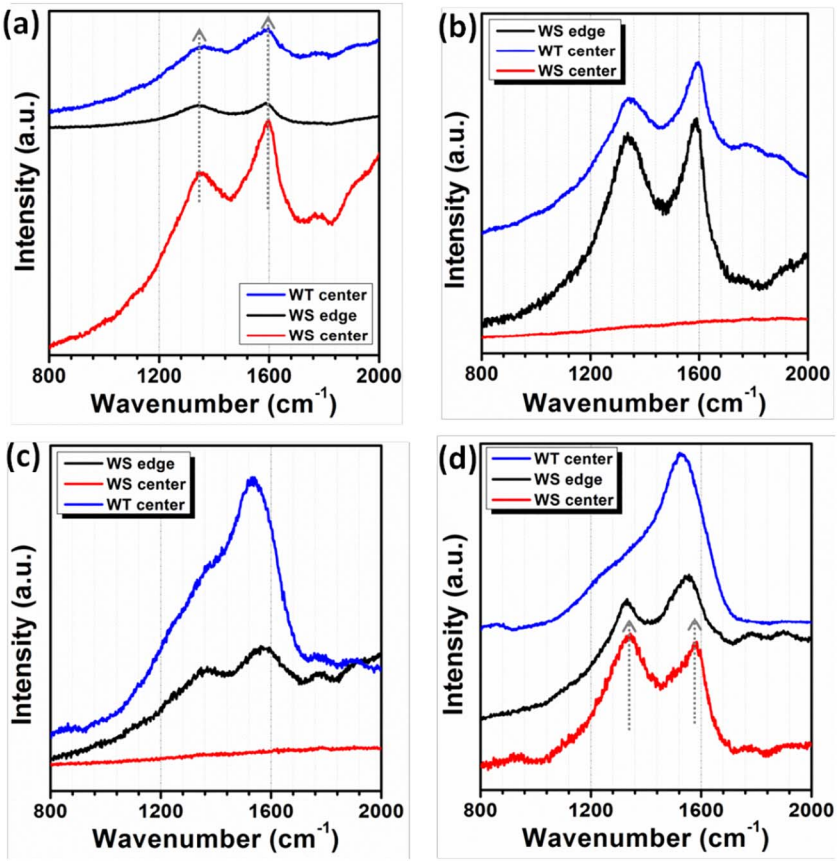

Fig. 6. Micro-Raman spectra of WT center, WS center and WS edge on uncoated Al_2O_3 surface in (a) dry nitrogen, (b) dry oxygen, (c) dry argon atmospheres and (d) on a-C:H coated Al_2O_3 surface in dry nitrogen. (WT: wear track, WS: wear scar).

off during the initial friction period and then was sprayed to the edge areas. In conclusion, both the Al_2O_3/a-C:H and self-mated a-C:H counterparts' ultra-low friction were attributed to the nitrogen terminal electrostatic repulsion and graphitic tribofilm.

3.3. XPS analysis of wear tracks

Although the friction coefficient of a-C:H film has been proved to be closely related to gas molecules' adsorption, its wear rates need to be further discussed. It seems that the wear rate had no direct relation with friction coefficient. For example, in Fig. 2 the wear rates of a-C:H in oxygen and humid air are approached, while their friction coefficients

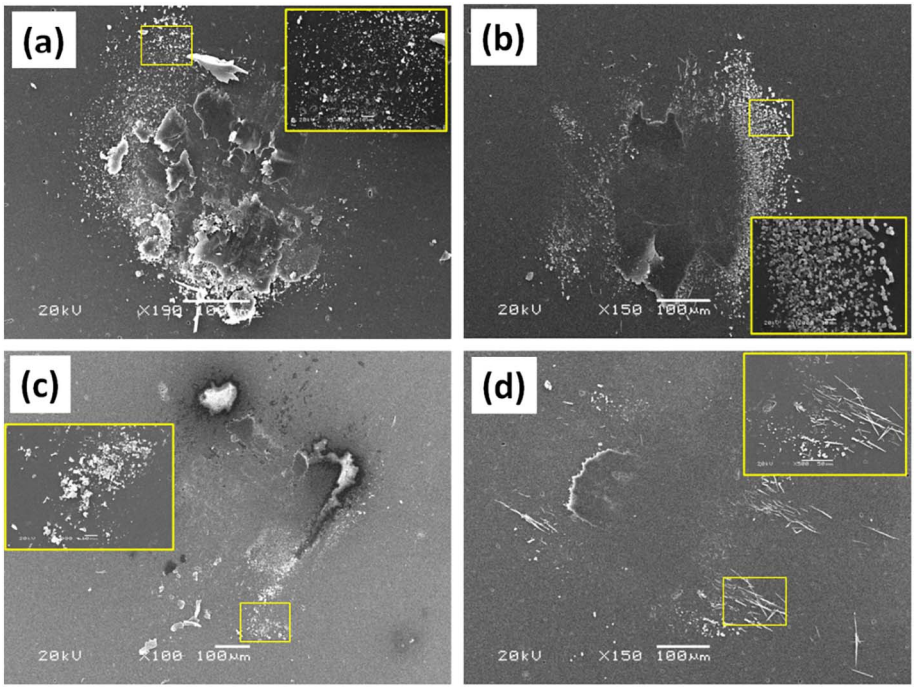

Fig. 7. SEM pictures of wear scar areas on uncoated Al_2O_3 balls sliding against a-C:H films in (a) N_2, (b) O_2, (c) Ar and (d) on coated Al_2O_3 surface in dry N_2 atmospheres. Insets show the corresponding enlarged SEM pictures of framed areas.

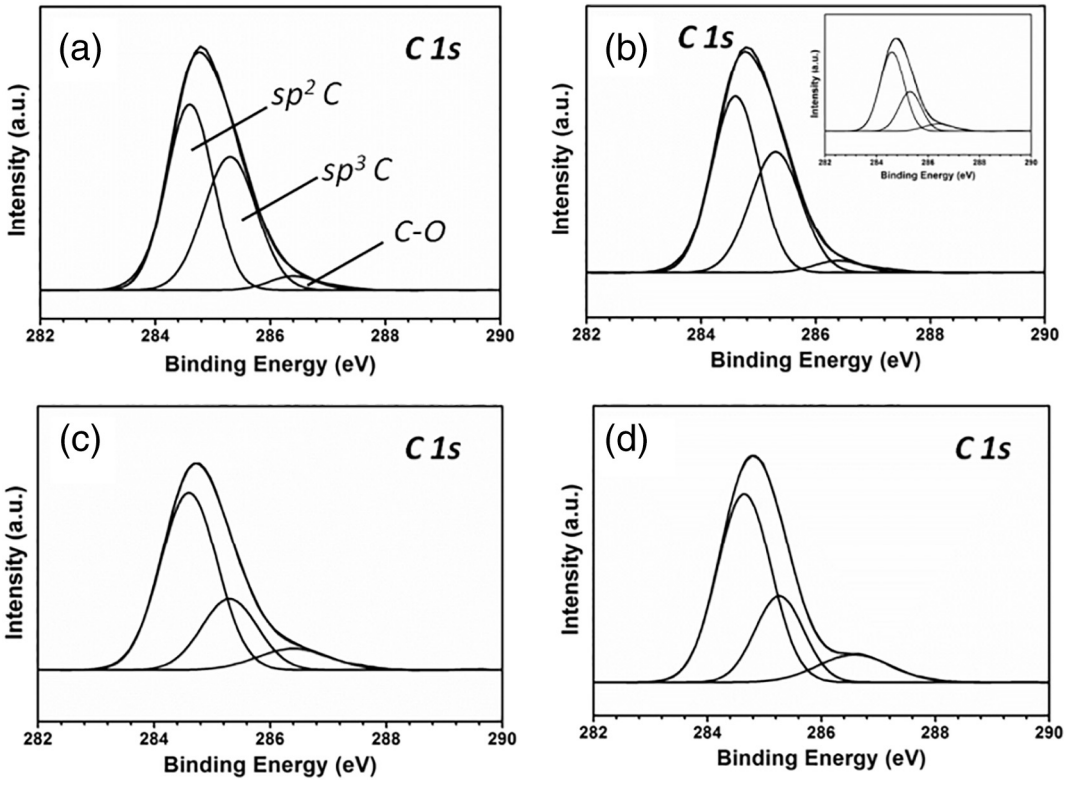

Fig. 8. Comparison of the C1s XPS spectrum of (a) as-deposited a-C:H bulk, (b) wear track center of a-C:H sliding against bare Al_2O_3 (inset shows self-mated a-C:H) in dry nitrogen, (c) in dry oxygen and (d) in dry argon.

have big difference. In this section, in order to get an insight into the effect of frictional interface chemical state change on wear rates, the XPS analysis was performed. The C1s spectra before and after friction tests were all shown in Fig. 8. The as-deposited bulk C1s spectrum was fitted into three components centered at 284.6 eV (sp^2 C), 285.3 eV (sp^3 C) and 286.4 eV (C—O bond), respectively (Fig. 8a) [22]. Here the ratio of deconvolution C—O peak to C1s peak was used to estimate the content of C—O bonds. Small amount of C—O bonds (4.0%) presented in the original film surface. This is because the film was moved out of the chamber after depositing and was exposed in air (Fig. 8a). In nitrogen atmosphere (Fig. 8b), this ratio of wear track centers for both bare Al_2O_3-as-pin (6.8%) and a-C:H coated Al_2O_3-as-pin (6%) show no obvious change compared with the original 4.0% ratio. Moreover, wear rates in these two conditions are $1.2 \times 10^{-8} mm^3 N^{-1} m^{-1}$ and $6.2 \times 10^{-9} mm^3 N^{-1} m^{-1}$, respectively. Therefore, the XPS analysis further proved that the adsorbed N_2 molecules serve as an adsorbed layer in boundary lubrication. On one hand, this protective layer acted as electron donator to provide low friction coefficient (Fig. 3) due to repulsion force. On the other hand, the wear rate in nitrogen (Fig. 3) was dramatically reduced because of this isolation effect. Similar C1s spectrum characteristic was found in argon atmosphere (Fig. 8d). This is because both nitrogen and argon molecules were not involved in tribo-oxidation reactions [25]. The difference between them is N_2 is physically adsorbed while Ar is barely adsorbed onto the film due to its electron orbits structure and just played a role in isolating the contact counterfaces. Therefore, both the friction coefficient and wear rate in Ar are higher than that in N_2 (shown in Fig. 3). Unlike the chemical inert nitrogen and argon, oxygen and H_2O molecules were adsorbed onto the shear stress freed C—C bonds to form abundant C—O bonds during sliding [56]. The C—O peak intensity obviously increased and the C—O bond ratio increased to 12.1% in oxygen (Fig. 8c). Peak fitting results in humid air (Fig. S4b) was similar to that of oxygen atmosphere and its C—O ratio was 12.7%. According to Kim et al., tribo-oxidation reaction was more severe in the presence of oxygen and water molecules [21,57]. Therefore, wear rates were higher in oxygen and humid air than that in nitrogen and argon atmospheres (Fig. 3), and the formation of tribofilms were destroyed easily (Fig. 7). It seems that the friction coefficient is profoundly affected by gas molecules adsorption while the tribo-oxidation is dominant for the wear rates [17,22,23,58]. In brief, the friction and wear behaviors of the a-C:H film in various atmospheres could be understood as follows. In dry nitrogen, repulsion force aroused by adsorption has a synergistic effect with graphitic tribofilm covered at wear scar center upon superlubricity. While in the presence of active species (oxygen and H_2O), the friction coefficient and wear rate were high due to strong adhesion aroused by chemical adsorption and the tribo-oxidation reaction [59,60]. Simultaneously, tribofilm at wear scar center was destroyed. However, argon molecules induced no tribo-oxidation reaction due to its chemical stability in electronic structure [61]. Therefore, the friction coefficient and wear rate in argon located between oxygen and nitrogen atmospheres. But in high vacuum, the generation of dangling bonds freed by shear stress was the main reason for its high friction coefficient and wear rate.

4. Conclusion

In this study, chemical vapor deposition prepared a-C:H film was revealed to have varied friction coefficient and wear rate in different atmospheres. Effect of physical and chemical state of frictional interface on its tribological property was discussed. From the comparison results of various atmospheres (N_2, O_2, Ar, humid air) and high vacuum friction, it was indicated that gas species have pronounced effect on a-C:H film's tribological properties. Physically adsorbed N_2 gas layer aroused repulsion force and provided superlubricity for self-mated a-C:H counterparts. Meanwhile, tribofilm has a synergistic effect with gas adsorption on superlubricity. Tribofilm at wear scar center in dry nitrogen experienced transformation of amorphous structure to sp^2 rich graphitic phase in small range. While in oxygen, argon and humid air, the tribofilm at wear scar center was destroyed easily. In the presence of

active species (oxygen and H_2O) both the friction and wear rate increased.

Acknowledgements

This work is supported by the Major State Basic Research Development Program of China (973 Program) (No 2013CB632304), the National Natural Science Foundation of China (Nos. 51575253 and 51365026).

Appendix A. Supplementary data

Supplementary data to this article can be found online at http://dx.doi.org/10.1016/j.diamond.2017.06.005.

References

[1] S. Akaike, D. Kobayashi, Y. Aono, M. Hiratsuka, A. Hirata, T. Hayakawa, Y. Nakamura, Relationship between static friction and surface wettability of orthodontic brackets coated with diamond-like carbon (DLC), fluorine- or silicone-doped DLC coatings, Diam. Relat. Mater. 61 (2016) 109–114.
[2] V.W. Wong, S.C. Tung, Overview of automotive engine friction and reduction trends - effects of surface, material, and lubricant-additive technologies, Friction 4 (2016) 1–28.
[3] J. Xu, J. Li, New achievements in superlubricity from international workshop on superlubricity: fundamental and applications, Friction 3 (2015) 344–351.
[4] D. Berman, S.A. Deshmukh, S.K.R.S. Sankaranarayanan, A. Erdemir, A.V. Sumant, Macroscale superlubricity enabled by graphene nanoscroll formation, Science 348 (2015) 1118–1122.
[5] A. Erdemir, O. Eryilmaz, Achieving superlubricity in DLC films by controlling bulk, surface, and tribochemistry, Friction 2 (2014) 140–155.
[6] A.Y. Wang, K.R. Lee, J.P. Ahn, J.H. Han, Structure and mechanical properties of W incorporated diamond-like carbon films prepared by a hybrid ion beam deposition technique, Carbon 44 (2006) 1826–1832.
[7] C.B. Wang, S.R. Yang, Q. Wang, Z. Wang, J.Y. Zhang, Super-low friction and superelastic hydrogenated carbon films originated from a unique fullerene-like nanostructure, Nanotechnology 19 (2008).
[8] Q. Wang, C.B. Wang, Z. Wang, J.Y. Zhang, D.Y. He, Fullerene nanostructure-induced excellent mechanical properties in hydrogenated amorphous carbon, Appl. Phys. Lett. 91 (2007).
[9] R.H. Zhang, L.P. Wang, Z.B. Lu, Probing the intrinsic failure mechanism of fluorinated amorphous carbon film based on the first-principles calculations, Sci. Rep. (2015) (Uk 5).
[10] A. Erdemir, C. Donnet, Tribology of diamond-like carbon films: recent progress and future prospects, J. Phys. D. Appl. Phys. 39 (2006) R311–R327.
[11] S.M. Ren, S.X. Zheng, J.B. Pu, Z.B. Lu, G.A. Zhang, Study of tribological mechanisms of carbon-based coatings in antiwear additive containing lubricants under high temperature, RSC Adv. 5 (2015) 66426–66437.
[12] A. Konicek, D. Grierson, A. Sumant, T. Friedmann, J. Sullivan, P. Gilbert, W. Sawyer, R.W. Carpick, Influence of surface passivation on the friction and wear behavior of ultrananocrystalline diamond and tetrahedral amorphous carbon thin films, Phys. Rev. B 85 (2012) 155448.
[13] T. Kunze, M. Posselt, S. Gemming, G. Seifert, A.R. Konicek, R.W. Carpick, L. Pastewka, M. Moseler, Wear, plasticity, and rehybridization in tetrahedral amorphous carbon, Tribol. Lett. 53 (2013) 119–126.
[14] J.M. Martin, M.I.D.B. Bouchet, C. Matta, Q. Zhang, W.A. Goddard, S. Okuda, T. Sagawa, Gas-phase lubrication of ta-C by glycerol and hydrogen peroxide. Experimental and computer modeling, J. Phys. Chem. C 114 (2010) 5003–5011.
[15] A.R. Konicek, D.S. Grierson, A.V. Sumant, T.A. Friedmann, J.P. Sullivan, P.U.P.A. Gilbert, W.G. Sawyer, R.W. Carpick, Influence of surface passivation on the friction and wear behavior of ultrananocrystalline diamond and tetrahedral amorphous carbon thin films, Phys. Rev. B 85 (2012).
[16] K.D. Koshigan, F. Mangolini, J.B. McClimon, B. Vacher, S. Bec, R.W. Carpick, J. Fontaine, Understanding the hydrogen and oxygen gas pressure dependence of the tribological properties of silicon oxide–doped hydrogenated amorphous carbon coatings, Carbon 93 (2015) 851–860.
[17] P.A. Romero, L. Pastewka, J. Von Lautz, M. Moseler, Surface passivation and boundary lubrication of self-mated tetrahedral amorphous carbon asperities under extreme tribological conditions, Friction 2 (2014) 193–208.
[18] J. Andersson, R.A. Erck, A. Erdemir, Frictional behavior of diamondlike carbon films in vacuum and under varying water vapor pressure, Surf. Coat. Technol. 163 (2003) 535–540.
[19] L. Cui, Z. Lu, L. Wang, Toward low friction in high vacuum for hydrogenated diamondlike carbon by tailoring sliding interface, ACS Appl. Mater. Interfaces 5 (2013) 5889–5893.
[20] Y. Wu, H. Li, L. Ji, Y. Ye, J. Chen, H. Zhou, Vacuum tribological properties of a-C:H film in relation to internal stress and applied load, Tribol. Int. 71 (2014) 82–87.
[21] A. Alazizi, A. Draskovics, G. Ramirez, A. Erdemir, S.H. Kim, Tribochemistry of carbon films in oxygen and humid environments: oxidative wear and galvanic corrosion, Langmuir 32 (2016) 1996–2004.
[22] H. Li, T. Xu, C. Wang, J. Chen, H. Zhou, H. Liu, Tribochemical effects on the friction and wear behaviors of diamond-like carbon film under high relative humidity condition, Tribol. Lett. 19 (2005) 231–238.
[23] P.F. Wang, M. Hirose, Y. Suzuki, K. Adachi, Carbon tribo-layer for super-low friction of amorphous carbon nitride coatings in inert gas environments, Surf. Coat. Technol. 221 (2013) 163–172.
[24] L. Cui, Z. Lu, L. Wang, Probing the low-friction mechanism of diamond-like carbon by varying of sliding velocity and vacuum pressure, Carbon 66 (2014) 259–266.
[25] J.A. Heimberg, K.J. Wahl, I.L. Singer, A. Erdemir, Superlow friction behavior of diamond-like carbon coatings: time and speed effects, Appl. Phys. Lett. 78 (2001) 2449–2451.
[26] S. Jahanmir, M. Beltzer, An adsorption model for friction in boundary lubrication, Asle Trans. 29 (1986) 423–430.
[27] J. Shi, Y.F. Wang, Z.B. Gong, B. Zhang, C.B. Wang, J.Y. Zhang, Nanocrystalline graphite formed at fullerene-like carbon film frictional interface, Adv. Mater. Interfaces 8 (2017).
[28] Z. Wang, J.Y. Zhang, Deposition of hard elastic hydrogenated fullerenelike carbon films, J. Appl. Phys. 109 (2011).
[29] J. Robertson, Diamond-like amorphous carbon, Mater. Sci. Eng. R 37 (2002) 129–281.
[30] M.J. Marino, E. Hsiao, Y.S. Chen, O.L. Eryilmaz, A. Erdemir, S.H. Kim, Understanding run-in behavior of diamond-like carbon friction and preventing diamond-like carbon wear in humid air, Langmuir 27 (2011) 12702–12708.
[31] A.A. Al-Azizi, O. Eryilmaz, A. Erdemir, S.H. Kim, Surface structure of hydrogenated diamond-like carbon: origin of run-in behavior prior to superlubricious interfacial shear, Langmuir 31 (2015) 1711–1721.
[32] X. Wang, P. Wang, S.R. Yang, J.Y. Zhang, Tribological behaviors of fullerene-like hydrogenated carbon (FL-C:H) film in different atmospheres sliding against Si3N4 ball, Wear 265 (2008) 1708–1713.
[33] J. Fontaine, J.L. Loubet, T. Le Mogne, A. Grill, Superlow friction of diamond-like carbon films: a relation to viscoplastic properties, Tribol. Lett. 17 (2004) 709–714.
[34] J. Andersson, R.A. Erck, A. Erdemir, Friction of diamond-like carbon films in different atmospheres, Wear 254 (2003) 1070–1075.
[35] A. Alazizi, A.J. Barthel, N.D. Surdyka, J. Luo, S.H. Kim, Vapors in the ambient—a complication in tribological studies or an engineering solution of tribological problems? Friction 3 (2015) 85–114.
[36] M. Lee, B. Kim, J. Kim, W. Jhe, Noncontact friction via capillary shear interaction at nanoscale, Nat. Commun. 6 (2015).
[37] E. Riedo, F. Levy, H. Brune, Kinetics of capillary condensation in nanoscopic sliding friction, Phys. Rev. Lett. 88 (2002).
[38] Y. Liu, A. Erdemir, E.I. Meletis, An investigation of the relationship between graphitization and frictional behavior of DLC coatings, Surf. Coat. Technol. 86-7 (1996) 564–568.
[39] A. Erdemir, The role of hydrogen in tribological properties of diamond-like carbon films, Surf. Coat. Technol. 146 (2001) 292–297.
[40] F.P. Bowden, J.E. Young, Friction of diamond, graphite, and carbon and the influence of surface films, Proc. R. Soc. London, Ser. A 208 (1951) 444–455.
[41] L.P. Wang, L.C. Cui, Z.B. Lu, H. Zhou, Understanding the unusual friction behavior of hydrogen-free diamond-like carbon films in oxygen atmosphere by first-principles calculations, Carbon 100 (2016) 556–563.
[42] S. Dag, S. Ciraci, Atomic scale study of superlow friction between hydrogenated diamond surfaces, Phys. Rev. B 70 (2004).
[43] S. Brunauer, P.H. Emmett, E. Teller, Adsorption of gases in multimolecular layers, J. Am. Chem. Soc. 60 (1938) 309–319.
[44] G. Halsey, Physical adsorption on non-uniform surfaces, J. Chem. Phys. 16 (1948) 931–937.
[45] F. Schedin, A.K. Geim, S.V. Morozov, E.W. Hill, P. Blake, M.I. Katsnelson, K.S. Novoselov, Detection of individual gas molecules adsorbed on graphene, Nat. Mater. 6 (2007) 652–655.
[46] A. Socoliuc, E. Gnecco, S. Maier, O. Pfeiffer, A. Baratoff, R. Bennewitz, E. Meyer, Atomic-scale control of friction by actuation of nanometer-sized contacts, Science 313 (2006) 207–210.
[47] J. Robertson, E.P. Oreilly, Electronic and atomic-structure of amorphous-carbon, Phys. Rev. B 35 (1987) 2946–2957.
[48] D. Beeman, J. Silverman, R. Lynds, M.R. Anderson, Modeling studies of amorphous-carbon, Phys. Rev. B 30 (1984) 870–875.
[49] T.B. Ma, L.F. Wang, Y.Z. Hu, X. Li, H. Wang, A shear localization mechanism for lubricity of amorphous carbon materials, Sci Rep 4 (2014) 3662.
[50] P. Wang, M. Hirose, Y. Suzuki, K. Adachi, Carbon tribo-layer for super-low friction of amorphous carbon nitride coatings in inert gas environments, Surf. Coat. Technol. 221 (2013) 163–172.
[51] L. Wang, R. Zhang, U. Jansson, N. Nedfors, A near-wearless and extremely long lifetime amorphous carbon film under high vacuum, Sci Rep 5 (2015) 11119.
[52] D.S. Wang, S.Y. Chang, Y.C. Huang, J.B. Wu, H.J. Lai, M.S. Leu, Nanoscopic observations of stress-induced formation of graphitic nanocrystallites at amorphous carbon surfaces, Carbon 74 (2014) 302–311.
[53] K. Hayashi, K. Tezuka, N. Ozawa, T. Shimazaki, K. Adachi, M. Kubo, Tribochemical reaction dynamics simulation of hydrogen on a diamond-like carbon surface based on tight-binding quantum chemical molecular dynamics, J. Phys. Chem. C 115 (2011) 22981–22986.
[54] J.C. Sanchez-Lopez, A. Erdemir, C. Donnet, T.C. Rojas, Friction-induced structural transformations of diamondlike carbon coatings under various atmospheres, Surf. Coat. Technol. 163 (2003) 444–450.
[55] A.A. Voevodin, A.W. Phelps, J.S. Zabinski, M.S. Donley, Friction induced phase transformation of pulsed laser deposited diamond-like carbon, Diam. Relat. Mater. 5 (1996) 1264–1269.

[56] M. Binggeli, C.M. Mate, Influence of capillary condensation of water on nano-tribology studied by force microscopy, Appl. Phys. Lett. 65 (1994) 415–417.
[57] A. Rusanov, R. Nevshupa, J. Fontaine, J.M. Martin, T. Le Mogne, V. Elinson, A. Lyamin, E. Roman, Probing the tribochemical degradation of hydrogenated amorphous carbon using mechanically stimulated gas emission spectroscopy, Carbon 81 (2015) 788–799.
[58] A. Alazizi, A.J. Barthel, N.D. Surdyka, J.W. Luo, S.H. Kim, Vapors in the ambient - a complication in tribological studies or an engineering solution of tribological problems? Friction 3 (2015) 85–114.
[59] J. Fontaine, T. Le Mogne, J.L. Loubet, M. Belin, Achieving superlow friction with hydrogenated amorphous carbon: some key requirements, Thin Solid Films 482 (2005) 99–108.
[60] O.L. Eryilmaz, A. Erdemir, TOF-SIMS and XPS characterization of diamond-like carbon films after tests in inert and oxidizing environments, Wear 265 (2008) 244–254.
[61] M.J. Marino, E. Hsiao, L.C. Bradley, O.L. Eryilmaz, A. Erdemir, S.H. Kim, Is ultra-low friction needed to prevent wear of diamond-like carbon (DLC)? An alcohol vapor lubrication study for stainless steel/DLC interface, Tribol. Lett. 42 (2011) 285–291.